Journal of Alloys and Compounds 509 (2011) 3476–3480

Contents lists available at ScienceDirect

Journal of Alloys and Compounds

journal homepage: www.elsevier.com/locate/jallcom

Microstructure and compressive properties of multiprincipal component AlCoCrFeNiC$_x$ alloys

J.M. Zhu, H.M. Fu, H.F. Zhang*, A.M. Wang, H. Li, Z.Q. Hu

Shenyang National Laboratory for Materials Science, Institute of Metal Research, Chinese Academy of Sciences, 72 Wenhua Road, Shenyang 110016, China

ARTICLE INFO

Article history:
Received 27 July 2010
Received in revised form 8 October 2010
Accepted 11 October 2010
Available online 23 October 2010

Keywords:
Multiprincipal component
Mechanical properties
Microstructure

ABSTRACT

By introducing nonmetallic carbon element, AlCoCrFeNiC$_x$ (x values in molar ratio, x = 0, 0.1, 0.2, 0.3, 0.4, 0.5, 1.0 and 1.5) alloys were designed and prepared. The effects of carbon element on microstructure and properties of as-cast AlCoCrFeNi alloy were investigated. It was found that the introduction of carbon element into AlCoCrFeNi alloy led to the formation of carbonization (ε phase) and compositional segregation in alloy. There was even graphite in alloy when carbon content was 1.0 and 1.5. The alloy strength was weakened to different extents when carbon content was between 0.1 and 0.5. The Young's modulus of alloy decreased largely when carbon content was 1.0 and 1.5, but the yield stress of alloy increased.

1. Introduction

In recent years, one kind of new alloys, high-entropy alloy with multiple principal elements in equimolar or near-equimolar ratios, has received more and more attentions due to its unique structure and excellent properties [1–7]. Promising properties in hardness, wear resistance, oxidation resistance and corrosion resistance can be obtained by proper composition design [4,8–10]. These discoveries bring new ideas to materials design and stimulate a new conception of materials research. A series of multiprincipal component alloy systems have been explored in the past decade [11–14]. The most commonly used elements are Al, Ti, Cr, Fe, Co, Ni and Cu. These elements except Al are transition metal elements of the fourth period. It is known that the proper addition of elements like C and Si with small atomic radii in traditional materials like steel is beneficial to their structure and properties [15–18]. However, the effects of nonmetallic elements on the multiprincipal component alloys are rarely investigated and reported. The effects of Si and Mo elements on AlCoCrFeNi alloy have been studied in two other works of us, and the effects of Ti element on AlCoCrFeNi alloy have been studied by Zhou [12,19,20]. In order to enrich multiprincipal element alloy field, and investigate the differences of effects of different alloying elements on microstructures and properties of AlCoCrFeNi alloy, the effects of carbon element on microstructure and properties of multiprincipal component AlCoCrFeNi alloy are investigated systematically in this paper. The introduction of carbon element changes the microstructures of alloy evidently, which further leads to the change of alloy properties. The structure evolution and property change of alloy are discussed in detail.

2. Experimental

Alloy ingots with nominal compositions of AlCoCrFeNiC$_x$ (x values in molar ratio, x = 0, 0.1, 0.2, 0.3, 0.4, 0.5, 1.0 and 1.5, denoted by C_0, $C_{0.1}$, $C_{0.2}$, $C_{0.3}$, $C_{0.4}$, $C_{0.5}$, $C_{1.0}$ and $C_{1.5}$, respectively) were prepared by arc melting a mixture of ultrasonically cleansed Al, Co, Cr, Fe, Ni and C (graphite) elements with a purity of above 99.9 wt% in a water-cooled copper hearth under Ti-gettered high purity argon atmosphere. The chemical homogeneity was realized by repeated melting at least four times. The proper amount of ingots were then remelted under high vacuum in a quartz tube by using an induction heating coil and injected through a nozzle with 0.5–1 mm in diameter into a copper mould with a cavity of Φ5 mm × 50 mm. The phases and microstructures were characterized using X-ray diffractometer (XRD, Philips PW1050, Cu Kα), scanning electron microscope (SEM, Hitachi S3400N) accompanied with energy dispersive spectrometer and transmission electron microscope (TEM, JEOL 2010, 200 kV). The end surfaces of compressive samples with 5 mm in diameter and 10 mm in length were polished on 2000 grit sand papers. The microstructure of alloy was revealed by etching in aqua regia. Thin slices from as-cast rods were used for preparing the TEM samples, which were ground and mechanically dimpled with a GATAN precision dimple grinder as well as used argon ion milling as the final thinning process by a GATAN precision ion polishing system (PIPS). Compression test was performed on an Instron 5582 test machine with a strain rate of 1×10^{-4} s^{-1}, a strain gauge was used. The elastic modulus was determined by fitting slope of elastic stage of compressive curve.

3. Results

Fig. 1 shows the XRD patterns of as-cast AlCoCrFeNiC$_x$ alloys. All alloys present BCC reflections, the reflections of carbonization (ε phase) appear with the introduction of carbon element. The relative intensity of ε phase gets stronger and stronger as carbon content increases, which suggests that the weight fraction of ε

* Corresponding author. Tel.: +86 24 23971783; fax: +86 24 23891320.
E-mail address: hfzhang@imr.ac.cn (H.F. Zhang).

0925-8388/$ – see front matter © 2011 Published by Elsevier B.V.
doi:10.1016/j.jallcom.2010.10.047

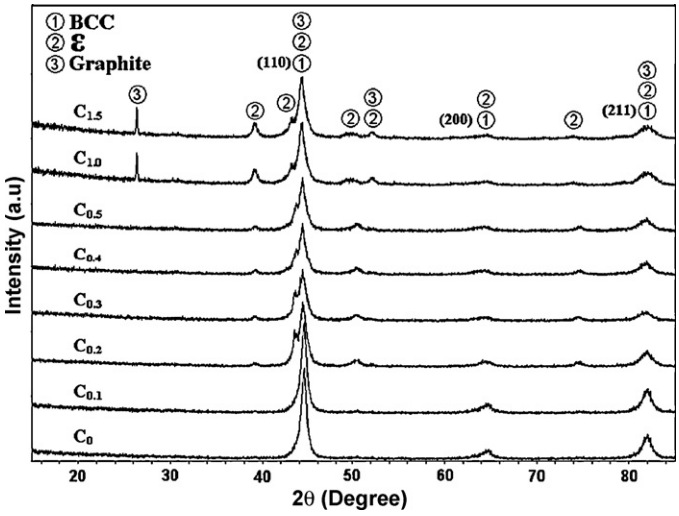

Fig. 1. XRD patterns of as-cast $AlCoCrFeNiC_x$ (x = 0, 0.1, 0.2, 0.3, 0.4, 0.5, 1.0 and 1.5) alloys.

phase increases. When the carbon content is 1.0 and 1.5, the reflections of graphite appear due to the excessive introduction of carbon element.

Fig. 2 shows the back-scattered images of as-cast $AlCoCrFeNiC_x$ alloys. It is seen that C_0 alloy exhibits single even featureless solid solution structure, which is consistent with the XRD result. When the carbon content is 0.1, the grain boundary of alloy becomes clear and coarse. The EDX results in Table 1 show that the grain boundary is rich in Cr and carbon elements. The molar ratio of elements except carbon in grain is close to each other. When the carbon content is 0.2, 0.3, 0.4 and 0.5, three distinct regions (A, B and C in Fig. 2(c–f)) in alloy are formed due to constitutional segregation. The EDX results show that region A is poor in Cr element, region B is poor in Al and Ni elements, and region C is rich in Cr and C elements. When the C content is 1.0 and 1.5, there are four distinct regions (A, B, C and D in Fig. 2(g and h)) in alloy. Graphite is identified in region D, which is consistent with the XRD results. In contrast with $C_{0.2}$, $C_{0.3}$, $C_{0.4}$ and $C_{0.5}$ alloys, the Cr content of region A in $C_{1.0}$ and $C_{1.5}$ alloys are higher than other elements. The composition of region B and C in $C_{1.0}$ and $C_{1.5}$ alloys are similar to those in $C_{0.2}$, $C_{0.3}$, $C_{0.4}$ and $C_{0.5}$ alloys.

Fig. 3 shows the TEM bright-field images with corresponding selected area electron diffraction (SAED) patterns of C_0, $C_{0.1}$, $C_{0.2}$ and $C_{1.5}$ alloys. Fig. 3(a) shows that C_0 alloy exhibits a single solid solution structure, which is consistent with the XRD and SEM results. The SAED pattern shown in Fig. 3(a) further confirms the single BCC structure of C_0 alloy. ε phase is observed in grain boundary of $C_{0.1}$ alloy, as shown in Fig. 3(b). The EDX results show that the ε phase is rich in Cr and carbon elements. The SAED pattern shown in Fig. 3(b) confirms the formation of ε phase. Similar to $C_{0.1}$ alloy, ε phase is also observed in $C_{0.2}$ and $C_{1.5}$ alloys, but it is found mainly in region C shown in Fig. 2(c and h).

Fig. 4 shows the room-temperature compressive true stress–strain curves of as-cast $AlCoCrFeNiC_x$ alloys. The Young's modulus E, yield strength σ_y, compressive fracture strength σ_{max} and plastic strain limit ε_p of the alloys are listed in Table 2. C_0 alloy exhibits good yield stress, plastic deformation and obvious work hardening behavior. The ductility of alloy is weakened as carbon content varies from 0 to 0.5 and 1.0 to1.5. The yield stress of alloy decreases as carbon content varies from 0 to 0.3, and then increases as carbon content varies from 0.3 to 1.5. The compressive strength of alloy decreases as carbon content varies from 0.1 to 0.3 and 0.4 to 1.5. The Young's modulus of $C_{0.1}$ is 213.2 GPa, which is much larger than 125.1 GPa of C_0 alloy. The Young's modulus of alloy decreases as carbon content varies from 0.1 to 0.3, and then increases as carbon varies from 0.3 to 0.5. The Young's modulus of alloy decreases largely when carbon content is 1.0 and 1.5. The compressive curves of $C_{0.1}$, $C_{0.2}$, $C_{0.3}$, $C_{0.4}$ and $C_{0.5}$ alloys are very similar, and the compressive curve of $C_{1.0}$ is similar to that of $C_{1.5}$ alloy. The work hardening behavior of $C_{0.4}$ and $C_{0.5}$ alloys are much obvious than those of $C_{0.1}$, $C_{0.2}$, $C_{0.3}$, $C_{1.0}$ and $C_{1.5}$ alloys.

Table 1
Compositions (at.%) of areas in as-cast $AlCoCrFeNiC_x$ (x = 0, 0.1, 0.2, 0.3, 0.4, 0.5, 1.0 and 1.5) alloys and atomic radii of different elements.

x	Areas in Fig 2	Al	Co	Cr	Fe	Ni	C
		1.43 Å	1.25 Å	1.21 Å	1.24 Å	1.24 Å	0.91 Å
0	Nominal	20.0	20.0	20.0	20.0	20.0	–
	EDX	16.7	21.1	21.2	21.9	19.1	–
0.1	Nominal	19.61	19.61	19.61	19.61	19.61	1.96
	Grain	13.08	14.04	12.29	14.73	13.38	32.02
	Boundary	7.50	10.06	28.42	13.19	7.16	33.68
0.2	Nominal	19.23	19.23	19.23	19.23	19.23	3.85
	A	14.36	15.47	8.70	13.35	17.02	31.10
	B	7.18	14.95	23.00	20.47	9.81	24.59
	C	2.43	5.15	38.70	8.07	3.80	41.85
0.3	Nominal	18.87	18.87	18.87	18.87	18.87	5.66
	A	21.68	15.86	5.38	12.11	19.88	25.27
	B	5.20	14.08	23.07	17.82	8.36	31.47
	C	0.03	2.20	47.06	6.67	0.65	43.38
0.4	Nominal	18.52	18.52	18.52	18.52	18.52	7.41
	A	18.20	13.33	3.39	10.98	16.83	37.26
	B	5.75	17.10	17.81	19.71	9.27	30.36
	C	0.08	3.16	47.35	7.31	0.89	41.22
0.5	Nominal	18.18	18.18	18.18	18.18	18.18	9.09
	A	20.52	14.24	2.84	10.73	19.13	32.53
	B	5.95	15.38	16.79	19.96	10.16	31.76
	C	0.09	3.60	42.84	7.07	0.77	45.63
1.0	Nominal	16.67	16.67	16.67	16.67	16.67	16.67
	A	12.24	13.21	24.74	14.32	14.24	21.26
	B	9.05	28.53	8.02	28.65	10.70	15.06
	C	1.10	3.50	41.84	7.17	0.98	45.71
	D	0.16	0.15	0.22	0.20	0.12	99.16
1.5	Nominal	15.38	15.38	15.38	15.38	15.38	23.08
	A	13.23	12.22	26.75	11.31	15.23	19.27
	B	5.85	21.49	16.65	26.91	9.66	19.44
	C	2.09	4.70	40.64	8.77	1.07	42.63
	D	0.09	0.22	0.49	0.36	0.24	98.60

4. Discussion

The effects of nonmetallic carbon element on AlCoCrFeNi alloy are neither similar to that of metallic Mo and Ti elements nor that of nonmetallic Si element. In $AlCoCrFeNiMo_y$ (y values in molar ratio, y = 0, 0.1, 0.2, 0.3, 0.4 and 0.5) alloy system, Mo element exists mainly in solid solution by substituting other element when Mo content is low. The alloy appears with eutectic reaction, which

Table 2
Mechanical properties of as-cast $AlCoCrFeNiC_x$ (x = 0, 0.1, 0.2, 0.3, 0.4, 0.5, 1.0 and 1.5) alloys.

x	Young's modulus E (GPa)	Yield stress σ_y (MPa)	Compressive strength σ_{max} (MPa)	Plastic strain ε_p (%)
0	125.1	1138	–	–
0.1	213.2	957	2550	10.52
0.2	150.9	906	2386	8.68
0.3	137.2	867	2178	7.82
0.4	156.1	1056	2375	6.67
0.5	180.8	1060	2250	5.60
1.0	75.1	1251	2166	7.04
1.5	72.5	1255	2083	5.54

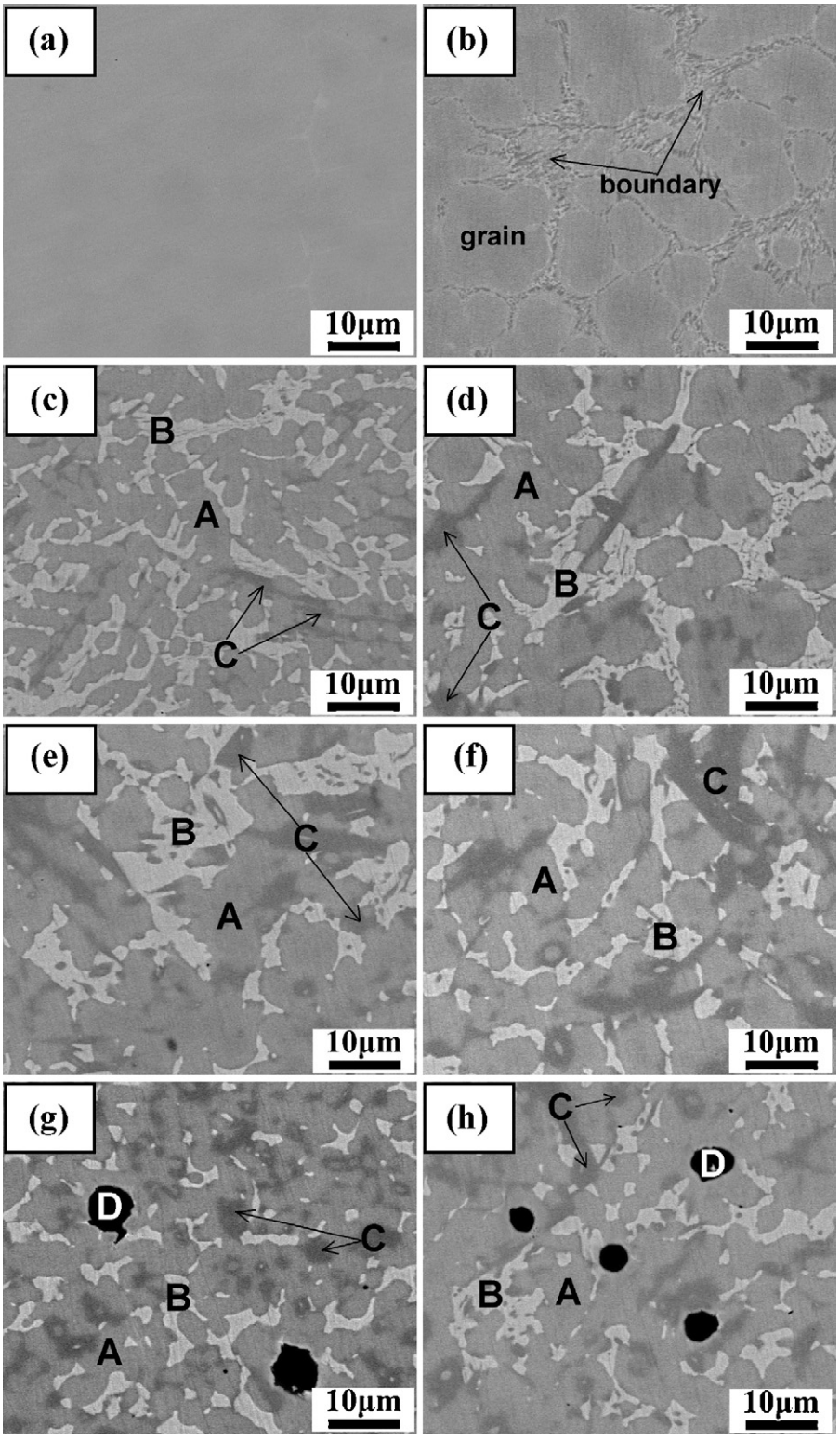

Fig. 2. Back-scattered images of as-cast $AlCoCrFeNiC_x$ alloys: (a) 0, (b) 0.1, (c) 0.2, (d) 0.3, (e) 0.4, (f) 0.5, (g) 1.0, (h) 1.5.

results in the formation of α phase, when Mo content is more than 0.1. In $AlCoCrFeNiTi_k$ (k values in molar ratio, $k = 0$, 0.5, 1.0 and 1.5) alloy system, the introduction of Ti element results in the precipitation of another BCC phase, which becomes the main phase. Laves phase identified as Fe_2Ti type forms in alloy when Ti content is 1.5. In $AlCoCrFeNiSi_m$ (m values in molar ratio, $m = 0$, 0.2, 0.4, 0.6, 0.8 and 1.0) alloy system, nanoscale cellular structure is precipitated in the grain of alloys with Si introduction through spinodal decomposition. δ phase forms at the grain boundary of alloy when Si content is between 0.6 and 1.0. Si element exists mainly in solid solution by substituting other elements.

According to the three principles for the formation of solid solution: (1) at least five components with equiatomic ratio, this meets the high entropy of mixing; (2) atomic radius difference is <12%;

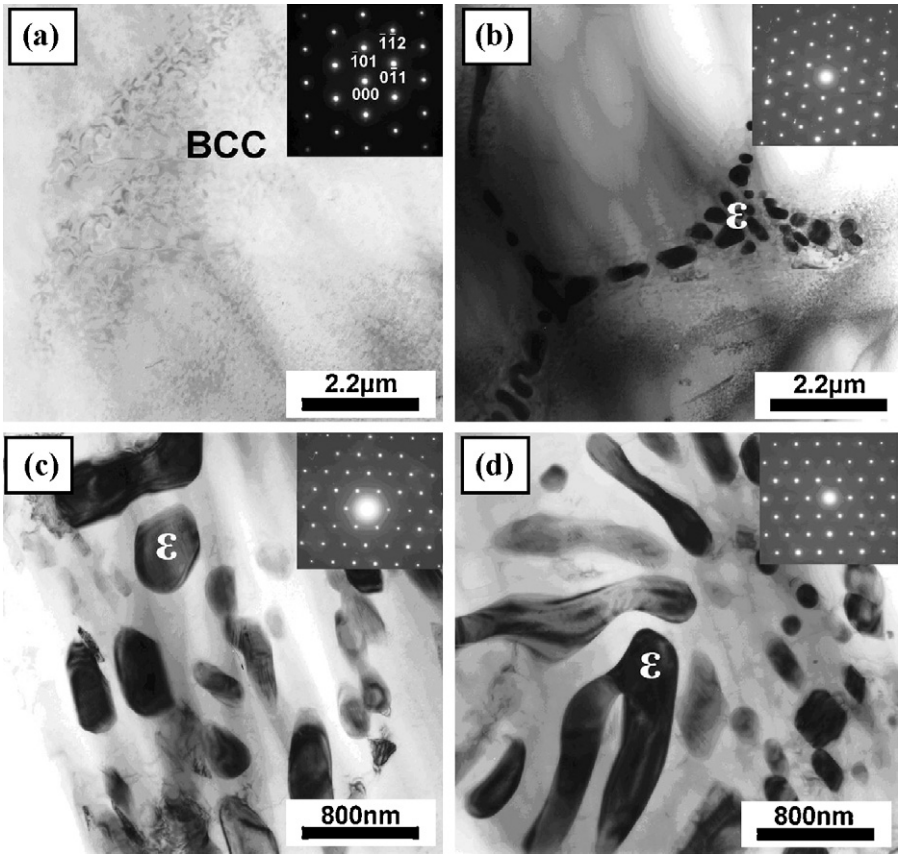

Fig. 3. TEM images with corresponding SAED patterns (inserted pictures) of as-cast $AlCoCrFeNiC_x$ alloys: (a) 0, (b) 0.1, (c) 0.2, (d) 1.5.

(3) enthalpy of mixing is in the range of −40 to 10 kJ/mol [21]. The atomic radii of elements in alloy are listed in Table 1. The atomic radius of carbon is far smaller than those of other elements in alloy. The mixing enthalpy values of C–Al, C–Co, C–Cr, C–Fe and C–Ni pairs are 17, 22, 21, 22 and 1 kJ/mol, respectively [22]. It is clear that these values are large positive. That is to say it is impossible for carbon element to exist mainly in solid solution by substituting other element. Moreover, the interstitial solid solubility of carbon element in alloy is quite limited, so carbon element can only exist mainly in alloy in the form of carbonization or graphite. In this research, the introduction of carbon element into AlCoCrFeNi alloy led to the formation of ε phase and compositional segregation in alloy. There is even graphite in alloy when carbon content is 1.0 and 1.5. However, the total number of phases is well below the maximum number of phases in equilibrium allowed by the Gibbs phase rule [23]. The prior formation of simple solid solutions to intermetallic compounds in this alloy system is attributed to the effect of high entropy of mixing [6].

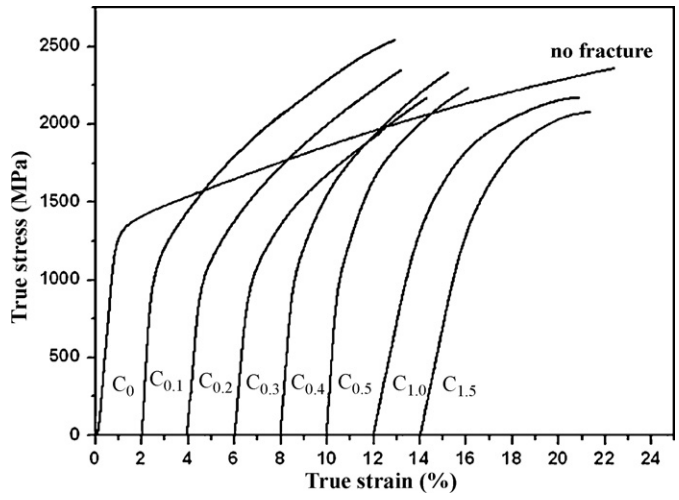

Fig. 4. Compressive true stress–strain curves of as-cast $AlCoCrFeNiC_x$ (x = 0, 0.1, 0.2, 0.3, 0.4, 0.5, 1.0 and 1.5) alloys.

The strength of AlCoCrFeNi alloy is increased to varying degrees by introducing Mo, Ti and Si elements, respectively. The strengthening mechanisms are attributed to solid solution and dispersion strengthening. The strength of $AlCoCrFeNiMo_y$ alloy increases as y increases from 0 to 0.5, but the ductility is weakened at the same time. Similar to $AlCoCrFeNiMo_y$ alloy, the strength of $AlCoCrFeNiSi_m$ alloy increases with the plasticity decreasing as m increases from 0 to 1.0. Among $AlCoCrFeNiTi_k$ alloys, $AlCoCrFeNiTi_{0.5}$ alloy exhibits the best mechanical properties. In $AlCoCrFeNiC_x$ alloy system, the alloy strength and ductility are weakened to different extent when carbon content is low. The yield stress of alloy increases when carbon content is 1.0 and 1.5, but the Young's modulus of alloy decreases largely at the same time. ε phase at the grain boundary of $C_{0.1}$ alloy and those distributed inhomogeneously in $C_{0.2}$, $C_{0.3}$, $C_{0.4}$, $C_{0.5}$, $C_{1.0}$ and $C_{1.5}$ alloys are responsible for the decreased alloy strength and ductility. Because the brittle ε phase at the grain boundary of $C_{0.1}$ alloy will result in intercrystalline rupture. The brittle ε phase distributed inhomogeneously in $C_{0.2}$, $C_{0.3}$, $C_{0.4}$, $C_{0.5}$, $C_{1.0}$ and $C_{1.5}$ alloys will result in inhomogeneous deformation of alloy, which will induce stress concentration in region C. The graphite observed in $C_{1.0}$ and $C_{1.5}$ may play certain roles in the decreased Young's modulus and increased yield stress of alloy.

5. Conclusions

The introduction of carbon element into AlCoCrFeNi alloy does not improve the mechanical properties of AlCoCrFeNi alloy obviously. Carbon element exists mainly in alloy in the form of carbonization or free carbon. The inhomogeneously distributed brittle ε phase and graphite in alloy are responsible for the decreased alloy strength and ductility.

Acknowledgment

The authors gratefully acknowledge the financial support from the National Natural Science Foundation of China (Grant No. 50825402)

References

[1] B. Cantor, I.Y.H. Chang, P. Knight, A.J.B. Vincent, Mater. Sci. Eng. (2004) 213, A375–377.
[2] J.W. Yeh, S.K. Chen, S.J. Lin, J.Y. Gan, T.S. Chin, T.T. Shun, C.H. Tsau, S.Y. Chang, Adv. Eng. Mater. 6 (2004) 299.
[3] S. Ranganathan, Curr. Sci. 85 (2003) 1404.
[4] P.K. Huang, J.W. Yeh, T.T. Shun, S.K. Chen, Adv. Eng. Mater. 6 (2004) 74.
[5] C.Y. Hsu, J.W. Yeh, S.K. Chen, T.T. Shun, Metall. Mater. Trans. A35 (2004) 1465.
[6] C.J. Tong, Y.L. Chen, S.K. Chen, J.W. Yeh, T.T. Shun, C.H. Tsau, S.J. Lin, S.Y. Chang, Metall. Mater. Trans. A36 (2005) 881.
[7] C.J. Tong, M.R. Chen, S.K. Chen, J.W. Yeh, T.T. Shun, S.J. Lin, S.Y. Chang, Metall. Mater. Trans. A36 (2005) 1263.
[8] Y.Y. Chen, T. Duval, U.D. Hung, J.W. Yeh, H.C. Shih, Corros. Sci. 47 (2005) 2257.
[9] J.M. Wu, S.J. Lin, J.W. Yeh, S.K. Chen, Y.S. Huang, H.C. Cheng, Wear 261 (2006) 513.
[10] T.K. Chen, T.T. Shun, J.W. Yeh, M.S. Wong, Surf. Coat. Technol. 188–189 (2004) 193.
[11] J.T. Chung, R.C. Chen, K.C. Swe, W.Y. Jien, T.S. Tao, J.L. Su, Y.C. Shou, Metall. Mater. Trans. A 35 (2004) 1465.
[12] Y.J. Zhou, Y. Zhang, Y. Wang, G.L. Chen, Appl. Phys. Lett. 90 (2007) 181904.
[13] J.H. Yu, C.C. Wen, K.W. Jiann, Mater. Chem. Phys. 112–117 (2005) 92.
[14] F.J. Wang, Y. Zhang, Mater. Sci. Eng. A 214–216 (2008) 496.
[15] M. Kondo, M. Takahashi, J. Nucl. Mater. 356 (2006) 203.
[16] D.Y. Lin, T.C. Chang, Mater. Sci. Eng. A 359 (2003) 396.
[17] M. Itabashi, K. Kawata, Int. J. Impact Eng. 24 (2000) 117.
[18] S.Z. Wei, J.H. Zhu, L.J. Xu, L. Rui, Mater. Des. 27 (2006) 58.
[19] J.M. Zhu, H.M. Fu, H.F. Zhang, A.M. Wang, H. Li, Z.Q. Hu, Mater. Sci. Eng. A 7210–7214 (2010) 527.
[20] J.M. Zhu, H.M. Fu, H.F. Zhang, A.M. Wang, H. Li, Z.Q. Hu, Mater. Sci. Eng. A 6975–6979 (2010) 527.
[21] J.Y. Yang, Y.J. Zhou, Y. Zhang, G.L. Chen, China Mater. Technol. Equipment 61 (2007) 5 (in Chinese).
[22] F.R. de Boom, W.C.M. Mattens, A.R. Miedema, A.K. Nissen, Cohesion in Metals, Elsevier Science Publishing Company, 1989.
[23] D. William Jr., Callister, Fundamentals of Materials Science and Engineering, John Wiley & Sons, New York, 2001.